Journal of Hazardous Materials 398 (2020) 122826

Contents lists available at ScienceDirect

Journal of Hazardous Materials

journal homepage: www.elsevier.com/locate/jhazmat

Comparison of the Fe^{2+}/H_2O_2 and Fe^{2+}/PMS systems in simulated sludge: Removal of PAHs, migration of elements and formation of chlorination by-products

Xiaojun Lai, Xun-an Ning*, Jiayi Chen, Yang Li, Yaping Zhang, Yiqian Yuan

Guangdong Key Laboratory of Environmental Catalysis and Health Risk Control, School of Environmental Science and Engineering, Institute of Environmental Health and Pollution Control, Guangdong University of Technology, Guangzhou 510006, China

GRAPHICAL ABSTRACT

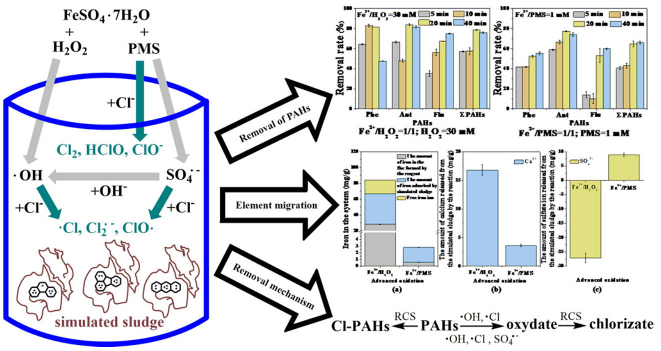

ARTICLE INFO

Editor: L. Eder

Keywords:
Textile dyeing sludge
Advanced oxidation process
Element migration
Polycyclic aromatic hydrocarbons (PAHs)
Chlorination by-product

ABSTRACT

In this study, polycyclic aromatic hydrocarbons (PAHs) at practical concentrations in the simulated sludge treated by the Fe^{2+}/H_2O_2 and Fe^{2+}/peroxymonosulfate (PMS) systems were evaluated in terms of the PAHs (phenanthrene, anthracene, fluoranthene) removal, element migration, Cl^- effect, and chlorination by-product formation. The results indicated that according to the removal rate of PAHs, the optimal dosage of the Fe^{2+}/PMS system (ΣPAHs removal rate was 64.66 ± 2.82 %) was 1/30 of that for the Fe^{2+}/H_2O_2 system (ΣPAHs removal rate was 78.63 ± 0.38 %). The elemental contents in the simulated sludge were mainly affected by the extent of advanced oxidation and the amount of generated iron flocs. By studying the PAHs removal, free chlorine formation, total organochlorine content, and PAHs products in $Fe^{2+}/H_2O_2/Cl^-$ and $Fe^{2+}/PMS/Cl^-$ systems, it was found that chlorine radicals (·Cl) had high reactivity with phenanthrene and fluoranthene, whereas dichloride anion radicals ($Cl_2^{\cdot-}$) exhibited the opposite behavior. Furthermore, PAHs were oxidized by ·Cl and hydroxyl radical in the $Fe^{2+}/H_2O_2/Cl^-$ system, whereas PAHs and their products were chlorinated by free chlorine and ·Cl in the $Fe^{2+}/PMS/Cl^-$ system to six chlorinated by-products such as Cl-PAHs (9-Cl-phenanthrene, 2-Cl-anthracene, 9,10-Cl_2-anthracene, 3-Cl-fluoranthene). These results provide some useful suggestions for the safe advanced oxidation process treatment of textile dyeing sludge.

---

* Corresponding author.
E-mail addresses: ningxunan666@126.com, 1009560924@qq.com (X.-a. Ning).

https://doi.org/10.1016/j.jhazmat.2020.122826
Received 10 February 2020; Received in revised form 23 April 2020; Accepted 23 April 2020
Available online 20 May 2020
0304-3894/ © 2020 Published by Elsevier B.V.

1. Introduction

Textile dyeing sludge has a complex composition and contains more than 500 types of organic compounds, including 91 priority pollutants such as chlorobenzene, phenolic compounds, polycyclic aromatic hydrocarbons (PAHs), aromatic amines, and other persistent organic pollutants (POPs) (Liang et al., 2013; Wang et al., 2011; Weng et al., 2012). The content of Σ_{16} PAHs in textile dyeing sludge was 1463 ± 177 ng/g to 16,714 ± 1507 ng/g, and the main components of PAHs were phenanthrene (Phe), anthracene (Ant), and fluoranthene (Flu) (Ning et al., 2014). Moreover, owing to the extensive use of flocculants such as ferric chloride, polyaluminum chloride and polymeric ferric sulfate (PFS), textile dyeing sludge has a large content of elements such as S, Cl, Fe, and Al (Zhang et al., 2017).

The traditional Fe^{2+}/H_2O_2 system is a commonly used advanced oxidation technology that has been investigated in several studies. For example, Lin et al. (2016) treated PAHs in textile dyeing sludge with Fe^{2+}/H_2O_2 and found that the removal rate of Σ_{16} PAHs reached 83.5 %. However, the production of a large amount of iron flocs by H_2O_2 and Fe^{2+} has limited the wide application of the Fe^{2+}/H_2O_2 system (Pignatello et al., 2006), and the dilution effect of iron flocs on organic matter has been rarely considered in the studies reported in the literature. In addition, the investigations of the Fe^{2+}/peroxymonosulfate (HSO_5^-, PMS) system have mainly focused on sludge dehydration (Liu et al., 2018). Although the degradation of trace organic pollutants (antibiotics, toluene) (Balcioglu et al., 2017; Oncu et al., 2015; Waclawek et al., 2016) in the sludge by activated PMS had attracted much attention, studies of the degradation of trace organic pollutants in the sludge by the Fe^{2+}/PMS system have been rare; thus, further investigations of the degradation of PAHs in textile dyeing sludge by the Fe^{2+}/PMS system are necessary.

The main oxidation radicals in the Fe^{2+}/H_2O_2 and Fe^{2+}/PMS systems are the hydroxyl radical (·OH) and the sulfate radical ($SO_4^{\cdot -}$); these radicals are non-selective and have oxidation potentials of 2.8 V and 2.5–3.1 V, respectively (Cai et al., 2014; Lin et al., 2014). The existence of Cl^- in textile dyeing sludge is inevitable, and in the degradation system, Cl^- not only forms free chlorine (Cl_2, HClO, ClO^-) with H_2O_2 and PMS, but also forms free radical reactive chlorine species (·Cl, $Cl_2^{\cdot -}$, ·ClO) with ·OH and $SO_4^{\cdot -}$ (Fang et al., 2014). Free chlorine and free radical reactive chlorine species are collectively referred to as reactive chlorine species (RCS). Free chlorine (Cl_2, HClO) chlorinated aromatic compounds (e.g. PAHs) and non-aromatic compounds through electrophilic substitution, and Cl_2 has stronger electrophilic ability than HClO (Georgi et al., 2007; Zhu et al., 2011). ·Cl, $Cl_2^{\cdot -}$ and ·ClO are selective radicals with oxidation potentials of 2.47, 2.0, and 1.5–1.8 V, respectively (Beitz et al., 1998). Free radical RCS can preferentially react with electron-rich moieties containing olefins, phenols, anilines, and alkyl-/alkoxybenzenes (Guo et al., 2017). Additionally, Cl^- may also be oxidized to form chlorate (ClO_3^-) (Hou et al., 2018). The study by Gu et al. (2018) showed that Cl^- were beneficial to the degradation of Phe by PMS system, proving that free radical RCS exhibited higher selective reaction of Phe. However, it is still necessary to further investigate which free radical RCS shows high reactivity with PAHs (Phe, Ant, Flu). Phthalic acid and phthalic anhydride were the main degradation products of Phe and Flu under the action of ·OH (Bendouz et al., 2017), and phthalic acid was converted into 1,2-benzenedicarboxylic acid dichloride when Cl^- were present in the PMS system (Yuan et al., 2011). Thus, either PAHs themselves or their degradation intermediates are likely to be chlorinated and then form chlorinated byproducts. However, previous studies had paid little attention to the effect of Cl^- on the PAHs degradation products. Therefore, it is necessary to study and compare the effects of Cl^- on the degradation of PAHs and the PAHs products in the Fe^{2+}/H_2O_2 and Fe^{2+}/PMS systems.

The advanced oxidation process will introduce a large amount of iron into the sludge, and may also change the contents of calcium, sulfur, phosphorus, and other elements in the sludge. This will affect the subsequent incineration of the sludge, which is currently the main method of its disposal (Zhang et al., 2013). Previous studies have shown that dioxin formation in the sludge thermochemical treatment was not only related to the chlorinated organics in sludge, but was also related to the $FeCl_3$, CaO, and S present in the sludge (Nganai et al., 2009; Qin et al., 2017). Therefore, it is necessary to compare the changes in the contents of iron, calcium, sulfur, and phosphorus in the simulated sludge degraded by the Fe^{2+}/H_2O_2 and Fe^{2+}/PMS systems, taking into account the entire sludge treatment and disposal process.

In this study, the Fe^{2+}/PMS system was applied to remove the main PAHs (Phe, Ant, Flu) in textile dyeing sludge, and the effects of the Fe^{2+}/H_2O_2 and Fe^{2+}/PMS systems for the removal of the PAHs (Phe, Ant, Flu) in the simulated sludge were compared. Then, the optimal conditions for the removal of PAHs (Phe, Ant, Flu) from the simulated sludge by the Fe^{2+}/H_2O_2 and Fe^{2+}/PMS systems were identified. Furthermore, based on the element migration observed for the simulated sludge, the effects of the Fe^{2+}/H_2O_2 and Fe^{2+}/PMS systems on subsequent sludge incineration disposal were examined. Finally, the effects of Cl^- on the removal of the PAHs (Phe, Ant, Flu) and PAHs (Phe, Ant, Flu) products by the Fe^{2+}/H_2O_2 and Fe^{2+}/PMS were studied. The price of $FeSO_4 \cdot 7H_2O$ is ¥9.0 per Kg, and the price of PMS (¥280.0 per Kg) is 127.27 times that of 30 % H_2O_2 (¥2.2 per Kg), so the actual usage of PMS cannot be equivalent to that of H_2O_2. It is more practical to compare the two systems under the optimal operating conditions and the same cost.

2. Materials and methods

2.1. Materials

Sources, purities and concentrations of chemicals are shown in Text S1.

2.2. Sludge samples and simulated sludge

Three types of textile dyeing sludge with a water content of 99 % were collected from three textile dyeing plants (TDP1-3) in different cities in Guangdong Province, China. The samples were refrigerated at 4 ℃ until analysis. The Cl^- contents in the water phase of the three types of textile dyeing sludge samples were 54.13 ± 4.77 mg/L (TDP1), 94.67 ± 2.38 mg/L (TDP2), and 1081.96 ± 14.31 mg/L (TDP3), respectively. The chemical composition of the solid phase of the textile dyeing sludge is shown in Fig. 1 and Text S2.

PFS solution was mixed with certain amounts of CaO (100 mesh), $Na_2HPO_4 \cdot 12H_2O$, and SiO_2. The mixture was continuously stirred with a magnetic stirrer (HMS-901D, China) at 200 rpm, and the pH was adjusted with a NaOH solution until pH = 7 (Lai et al., 2019; Liang et al., 2019). Then, the mixture was centrifuged at 4000 rpm for 10 min,

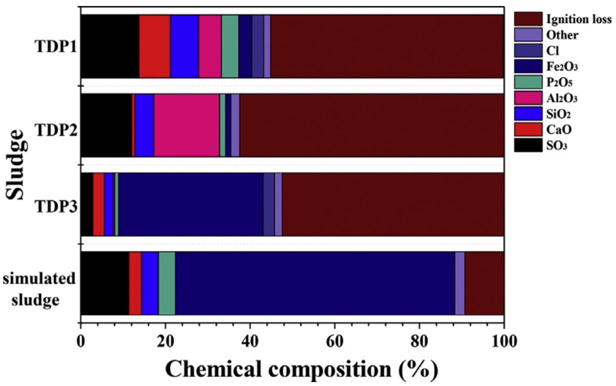

Fig. 1. Chemical composition of the textile dyeing sludge and the simulated sludge.

and the solid residue was freeze-dried (LGJ-10C, China) at −60 ℃ for 24 h. Finally, the simulated sludge that did not contain PAHs and had a similar physical structure and inorganic composition to the actual textile dyeing sludge was obtained. The chemical composition of the simulated sludge is shown in Fig. 1. X-ray fluorescence (XRF) spectrometer test shows that the relative contents (expressed in oxide form) of Fe, P, Si, Ca, and S in the simulated sludge were 65.97 %, 4.02 %, 3.96 %, 3.03 %, and 11.36 %, respectively. Iron ions in the simulated sludge might exist as hexaaquo ions ($Fe(H_2O)_6^{3+}$) (Bolobajev et al., 2016), and the simulated sludge did not contain Fe_2O_3, Fe_3O_4 and Fe° (Liang et al., 2019).

2.3. Experimental procedure

Details related to the experimental procedure are provided in the Text S3.

2.4. Analytical methods

Details pertaining to analytical methods are provided in the Text S4.

2.5. Quality assurance and quality control

Details pertaining to quality assurance and quality control are provided in the Text S5.

3. Results and discussion

3.1. Effects of different reagent ratios, reagent dosage and reaction time on PAHs removal

The effects of the reagent ratio, reagent dosage, and reaction time on the removal of PAHs by Fe^{2+}/H_2O_2 are shown in Fig. 2(a)–(c), respectively. According to Fig. 2(a), as the amount of Fe^{2+} increased, the ratio of Fe^{2+} to H_2O_2 increased, and the removal rates of Phe, Ant, and Flu increased. For the Fe^{2+} to H_2O_2 ratio higher than 1, the removal rate of the total PAHs did not increase significantly, so that the optimal Fe^{2+} to H_2O_2 mole ratio was identified as 1:1, which was similar to the research results of Lin et al. (2016) using Fe^{2+}/H_2O_2 to degrade PAHs in textile dyeing sludge. At these conditions, the removal rates of Phe, Ant, Flu, and total PAHs were 69.06 ± 4.00 %, 79.23 ± 0.80 %, 71.64 ± 0.05 %, and 76.58 ± 0.80 %, respectively. However, a large amount of iron flocs produced by the Fe^{2+}/H_2O_2 system increased the total amount of the sludge, diluting the organic matter in the sludge rather than removing it. Therefore, the removal rates of the PAHs after removing the influence of the iron flocs produced by the Fe^{2+}/H_2O_2 system is shown in Fig. S1. Comparing Fig. 2(a) with Fig. S1, it can be seen that when the dosage of Fe^{2+} is 11.11–33.33 mM, the total PAHs removal rate increases by 0.38–1.11 % due to dilution of iron flocs; when the dosage of Fe^{2+} is 100 mM and 150 mM, the total PAHs removal rate increases by 2.58 % and 4.00 % due to dilution of iron flocs. Therefore, when the amount of the added Fe^{2+} was less than 33.33 mM, the effect of the iron flocs produced by the Fe^{2+}/H_2O_2 system could be ignored.

As observed from Fig. 2(b), the removal rates of Phe, Ant, and Flu increased with increasing reagent dosage. The main components of PAHs in textile dyeing sludge were Phe, Ant and Flu (Ning et al., 2014), so the optimal dosage of degradation system should be determined according to the removal rate of total PAHs. As shown in Fig. 2(b), for the dosage of more than 30 mM, the removal rate of the total PAHs did not increase significantly—considering the interference of large error of Ant removal rate. Moreover, when the added Fe^{2+} was more than 30 mM, the increase of total PAHs removal rate (0.55–3.25 %) was probably due to dilution of iron flocs. Therefore, the optimal dosage was identified as 30 mM. At these conditions, the removal rates of Phe, Ant, Flu, and total PAHs were 47.53 ± 0.09 %, 81.69 ± 1.32 %, 74.96 ± 0.39 %, and 76.03 ± 0.61 %, respectively.

As shown in Fig. 2(c), the removal rates of Ant and Flu increased with longer reaction time. The decrease of Phe removal rate at 40 min might be due to the cracking of the simulated sludge, which might lead to the release of PAHs that were not originally detected in the simulated sludge, or the degradation of macromolecular PAHs to form small molecular PAHs (Bissey et al., 2006; Lin et al., 2016). When the reaction time was greater than 20 min, the removal rate of the total PAHs did not increase significantly, so that 20 min was determined to be the optimal reaction time. Based on the above-described results, the

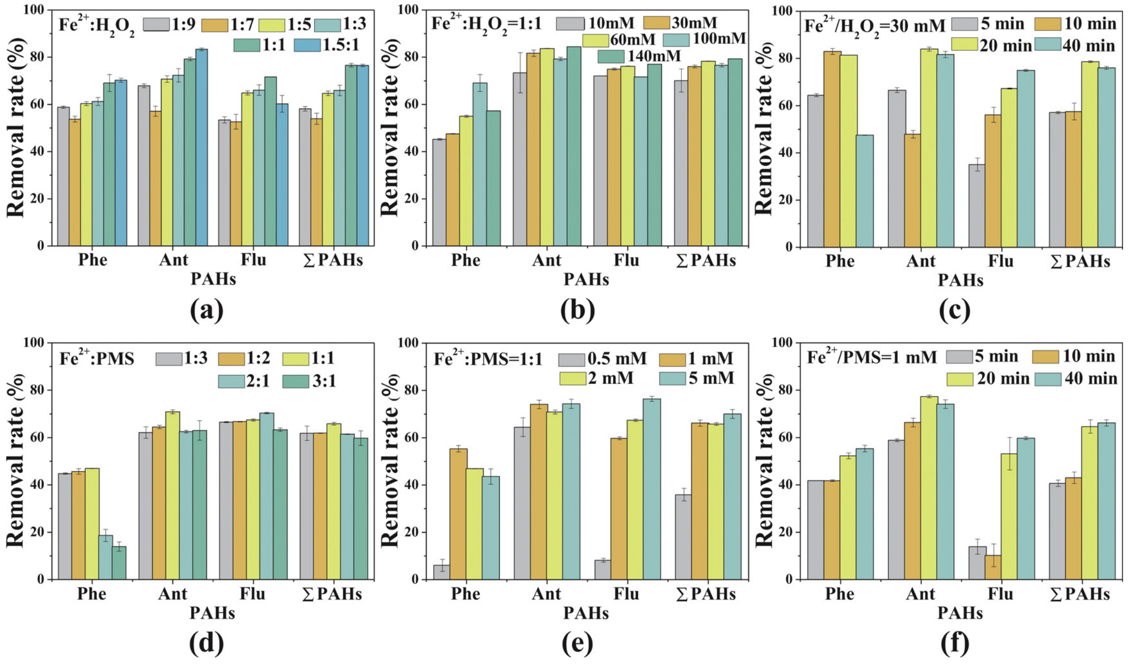

Fig. 2. Effects of reagent ratio, reagent dosage, and reaction time on removal of PAHs in simulated sludge by Fe^{2+}/H_2O_2 or Fe^{2+}/PMS (a: 100 mM H_2O_2, 40 min; b: Fe^{2+}/H_2O_2 = 1:1, 40 min; c: Fe^{2+}/H_2O_2 = 1:1, 30 mM H_2O_2; d: 2 mM PMS, 40 min; e: Fe^{2+}/PMS = 1:1, 40 min; f: Fe^{2+}/PMS = 1:1, 1 mM PMS).

optimal operating parameters for the removal of PAHs by the Fe^{2+}/H_2O_2 process (Fe^{2+}/H_2O_2 = 1:1, H_2O_2 = 30 mM, 20 min) were obtained. For these conditions, the removal rates of Phe, Ant, Flu, and total PAHs were 81.42 ± 0.07 %, 84.00 ± 0.88 %, 67.27 ± 0.22 %, and 78.63 ± 0.38 %, respectively.

The effects of the reagent ratio, reagent dosage, and reaction time on the removal of PAHs by the Fe^{2+}/PMS are shown in Fig. 2(d)–(f). When the Fe^{2+} to PMS mole ratio was greater than 1, or when the dosage was greater than 1 mM, or when the reaction time was greater than 20 min, the removal rate of total PAHs did not increase significantly. Thus, the dosage of PMS and Fe^{2+} of 1 mM, and the reaction time of 20 min were identified as the favorable conditions for the removal of PAHs. At these conditions, the removal rates of Phe, Ant, Flu, and total PAHs were 52.29 ± 1.21 %, 77.34 ± 0.59 %, 53.17 ± 6.88 %, and 64.66 ± 2.82 %, respectively.

According to Fig. 2, the removal efficiencies of PAHs were obtained in the order of Ant > Flu > Phe. This is due to the low energy required for the formation of a highly stable oxide (9,10-anthraquinone) in Ant degradation (Forsey et al., 2010). Moreover, Peluffo et al. (2016) found that Phe was the most difficult to degrade in the 3–4 rings PAHs. According to the price of reagents in China, the price of treating simulated sludge containing PAHs with the optimal conditions of the Fe^{2+}/H_2O_2 system (Fe^{2+}/H_2O_2 = 1:1, H_2O_2 = 30 mM, 20 min) is ¥82.54 per m^3; the price of treating simulated sludge containing PAHs with the optimal conditions of the Fe^{2+}/PMS system (Fe^{2+}/PMS = 1:1, PMS = 1 mM, 20 min) is ¥174.65 per m^3. Therefore, when the optimal dosage of the Fe^{2+}/PMS system was 1/30 of that for the Fe^{2+}/H_2O_2 system, the removal rate of the total PAHs was reduced by 13.97 %, and the treatment price was doubled. When the dosage of the Fe^{2+}/PMS (1:1) system was 0.5 mM (the removal rate of total PAHs was 35.93 ± 2.68 %; 40 min) and the dosage of the Fe^{2+}/H_2O_2 (1:1) system was 30 mM (the removal rate of total PAHs was 76.03 ± 0.61 %; 40 min), the cost of treating simulated sludge by the two systems was not much different. However, under these conditions, the removal rate of total PAHs by the Fe^{2+}/H_2O_2 (1:1; 30 mM) system was 2.11 times that by the Fe^{2+}/PMS (1:1; 0.5 mM) system. When the Fe^{2+}/H_2O_2 (1:1) system dosage was 10 mM (the removal rate of total PAHs was 70.10 ± 4.91 %) and the Fe^{2+}/PMS (1:1) system dosage was 5 mM (the removal rate of the total PAHs was 70.10 ± 1.87 %), the removal rates of the total PAHs in the two systems were equivalent. However, under these conditions, the treatment price of the Fe^{2+}/PMS (1:1; 5 mM) system was 31.74 times that of the Fe^{2+}/H_2O_2 (1:1; 10 mM) system. In conclusion, considering the removal of PAHs and the dosage and price of reagents, Fe^{2+}/H_2O_2 system was more advantageous for the removal of PAHs from the sludge.

3.2. Elemental migration in the Fe^{2+}/H_2O_2 and Fe^{2+}/PMS systems

Under the conditions of different iron ion dosage, the results for the migration of iron, calcium, and sulfur elements are shown in Fig. 3, and the pH before and after the reaction is shown in Table S1. The attribution of iron elements in the simulated sludge system was obtained by measuring the concentration of iron ions in the liquid phase of the degraded simulated sludge system and the degraded pure water system. Fig. 3(a) shows that the added Fe^{2+} formed a large amount of flocs ($[Fe_2(H_2O_4)(OH)_2]^{4+}$, $[Fe_2(H_2O_7)(OH)_3]^{3+}$, $[Fe_3(H_2O)_{10}(OH)_4]^{5+}$) in the Fe^{2+}/H_2O_2 system (Wang and Xu, 2003). With the increase of $FeSO_4{\cdot}7H_2O$ dosage, the particle size of iron-forming flocs increased (Zhang et al., 2005). Iron-forming flocs accounted for 28.98 %–50.43 % of the total added iron. When the addition of the $FeSO_4{\cdot}7H_2O$ was greater than 20 mM, iron ions appeared in the liquid phase, causing secondary pollution to the water environment. As shown in Fig. 3(d), Fe^{2+} added in Fe^{2+}/PMS system formed a small amount of flocs. Iron-forming flocs accounted for 0.36 %–32.41 % of the total added iron. No iron ions appeared in the liquid phase of the Fe^{2+}/PMS system. Fig. 3(a) and (d) shows that the simulated sludge can adsorb iron ions. When the Fe^{2+} dosage was greater than 20 mM, free iron appeared in the liquid phase, while when the dosage of Fe^{2+} was greater than 33.33 mM and the iron ion concentration of non-flocs was greater than 60.50 mg/g, the simulated sludge approached the limit of iron ion adsorption. The maximum amount of iron ions adsorbed by the simulated sludge was 38.5 mg/g. Simulated sludge is a floc with the ability to adsorb metal ions (Gang et al., 2019), so simulated sludge can adsorb iron ions. Lai et al. (2019) showed that the addition of sulfate greatly increased the specific surface area of simulated sludge, decreased the particle size of simulated sludge and increased the adsorption sites of simulated sludge. Therefore, in this experiment, with the increase of $FeSO_4{\cdot}7H_2O$ dosage, the ability of simulated sludge to adsorb iron ions was enhanced.

Bolobajev et al. (2016) showed that iron-containing sludge had a lower catalytic capacity for H_2O_2 than Fe^{3+}, because the release of iron from sludge into the aqueous medium required additional chemical reactions (protonation). In this study, the iron ions released by the simulated sludge were smaller than those adsorbed by the simulated sludge (Fig. 3(a) and (d)). Therefore, the activation of H_2O_2 and PMS would not be affected by iron ions released by simulated sludge.

As shown in Fig. 3(b) and (e), the Ca^{2+} ions in the simulated sludge were released into the water phase under the action of the Fe^{2+}/H_2O_2 or Fe^{2+}/PMS systems. In the Fe^{2+}/H_2O_2 system, the release of Ca^{2+} first increased and then decreased with the increase in the Fe^{2+} dosage. When the Fe^{2+} to H_2O_2 molar ratio was 1:3, the maximum Ca^{2+} release amount of 16.26 ± 1.11 mg/g was obtained. This may be because with the increase in the Fe^{2+} to H_2O_2 molar ratio, the Fe^{2+}/H_2O_2 reaction strengthened and the pH decreased (Table S1), increasing the release of Ca^{2+} from the simulated sludge. However, with the increased amount of added Fe^{2+}, a large amount of iron flocs were formed. Ca^{2+} can be adsorbed by these iron flocs, possibly explaining the observed reduction in the observed amount of released Ca^{2+}. In the Fe^{2+}/PMS system, the amount of released Ca^{2+} increased with the increase in the Fe^{2+} dosage. It is also likely that the pH decreased with the increase in the Fe^{2+} dosage (Table S1), enabling the $Ca(OH)_2$ in the simulated sludge to dissolve more Ca^{2+}.

The migration of sulfur in simulated sludge was obtained by measuring SO_4^{2-} concentration in the liquid phase of the degraded simulated sludge system and the degraded pure water system. The results for the migration of sulfur are shown in Fig. 3(c) and (f). In the Fe^{2+}/H_2O_2 system, with the increase in the Fe^{2+} dosage, SO_4^{2-} were first released from the simulated sludge and then were adsorbed by the iron flocs. Initially, the enhanced Fe^{2+}/H_2O_2 reaction increased the amount of the SO_4^{2-} released in the simulated sludge. However, with the increased amount of added Fe^{2+}, the amount of SO_4^{2-} adsorbed by the iron flocs was larger than that released by the simulated sludge, consistent with the results obtained for Ca^{2+} in the Fe^{2+}/H_2O_2 system. In the Fe^{2+}/PMS system, with the increase in the Fe^{2+} dosage, the amount of iron ions adsorbed by the simulated sludge increased and the mobility of SO_4^{2-} decreased, which was contrary to the results of Ca^{2+} in the Fe^{2+}/PMS system. Among them, when the molar ratio of Fe^{2+} to PMS was 2, the release of SO_4^{2-} suddenly increases, probably because the pH of the simulated sludge system was less than 5 (Table S1), which greatly reduced the stability of the simulated sludge (Cao et al., 2010). When the molar ratio of Fe^{2+} to PMS was 3, the simulated sludge adsorbed a large amount of iron ions, which improved the stability of simulated sludge or the ability of the simulated sludge to adsorb SO_4^{2-} (electrostatic adsorption), thus reducing the release of SO_4^{2-}. In addition, the phosphorus in the simulated sludge was not released in any of the reactions.

Based on the above experiments, the optimal reaction conditions for the removal of PAHs from simulated sludge were determined. Under the optimal reaction conditions (Fe^{2+}/H_2O_2 conditions: Fe^{2+}/H_2O_2 = 1:1, H_2O_2 = 30 mM, 20 min; Fe^{2+}/PMS conditions: Fe^{2+}/PMS = 1:1, PMS = 1 mM, 20 min), the migration of iron, calcium, and sulfur elements was continuously studied. As shown in Fig. 4, there were no iron

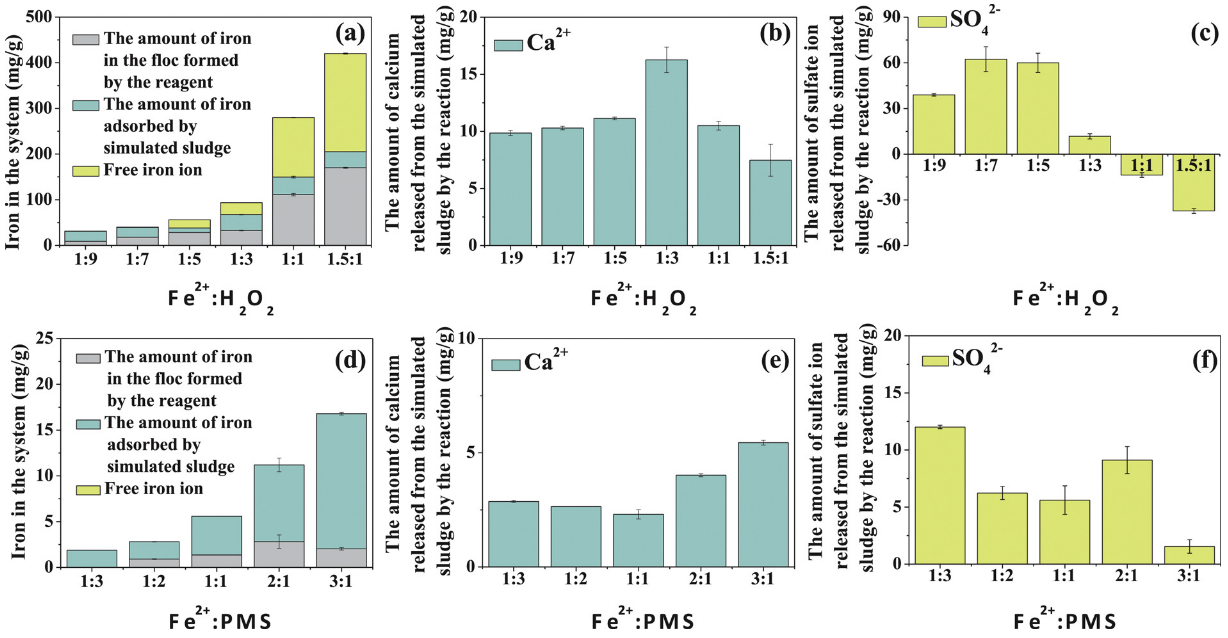

Fig. 3. Migration of iron, calcium and sulfur elements with different iron ion dosages (a,b,c: 100 mM H_2O_2, 40 min; d,e,f: 2 mM PMS, 40 min).

ions in the liquid phase of the Fe^{2+}/PMS system and no secondary pollution to the water environment was observed. Moreover, the amount of iron transferred into simulated sludge in the Fe^{2+}/H_2O_2 system was 23.83 times that in the Fe^{2+}/PMS system. The migration of Ca^{2+} in the Fe^{2+}/H_2O_2 system was 4.69 times that in the Fe^{2+}/PMS system, and the sulfur in the simulated sludge was released into the water phase after the treatment by the Fe^{2+}/PMS system instead of being adsorbed. Since most of the dehydrated sludge will be incinerated (Zhang et al., 2013), the influence of the content change of the characteristic elements after conditioning on the subsequent sludge incineration should also be considered. Sulfur in the sludge will produce sulfur dioxide during incineration, causing air pollution (Amand and Kassman, 2013). In addition, the CaO in the sludge is conducive to inhibiting dioxin formation during incineration (Qin et al., 2017), while iron oxide in the sludge catalyzes the conversion of dioxin precursors into dioxins (Nganai et al., 2009). Therefore, based on the results for the migration of the elements in the sludge, the textile dyeing sludge treated by the Fe^{2+}/PMS system is likely to give rise to less pollution in its subsequent incineration.

3.3. Effect of chloride ion on the Fe^{2+}/H_2O_2 and Fe^{2+}/PMS systems

Although the Cl^- concentration in the liquid phase of the three types of actual textile dyeing sludge was 54.13–1081.96 mg/L, some wastewater treatment plants use polymeric chloride as the flocculant; this greatly increases the Cl^- content in the solid and liquid phases of the sludge. Therefore, the Cl^- concentration range in this experiment was set to 0–5000 mg/L. The results for the effect of the Cl^- concentration on the removal of PAHs by the Fe^{2+}/H_2O_2 and Fe^{2+}/PMS systems are shown in Fig. 5(a) and (b). In the Fe^{2+}/H_2O_2 system, with the increase in the Cl^- concentration, the removal of Phe, Flu, and total PAHs first increased and then decreased. The removal rate of Ant decreased with increasing Cl^- concentration. The highest removal rate of total PAHs (80.93 % ± 1.09 %) was obtained for the Cl^- concentration of 50 mg/L,

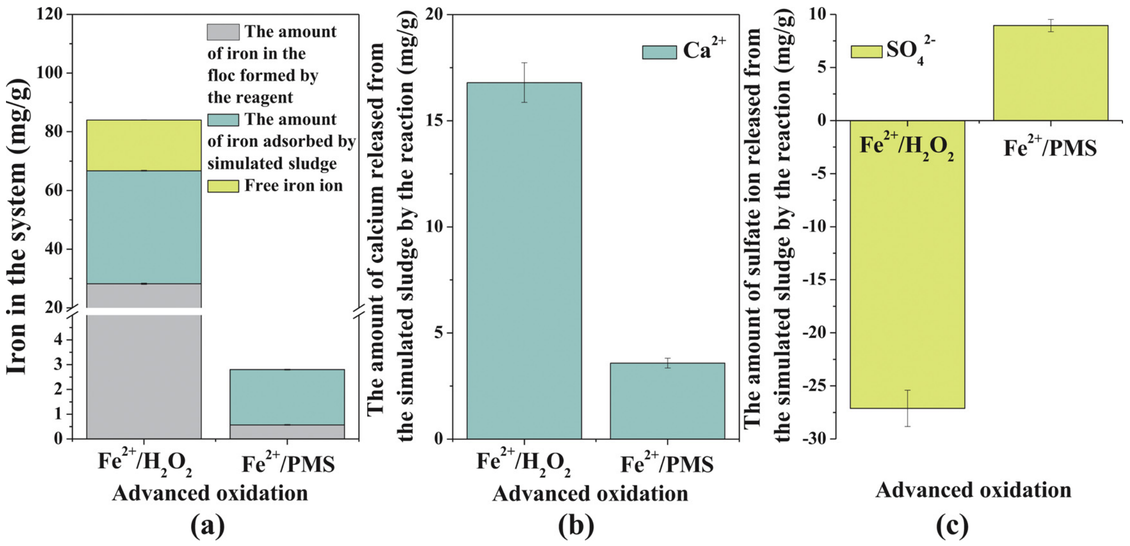

Fig. 4. Migration of iron, calcium, and sulfur elements under optimal treatment conditions (Fe^{2+}/H_2O_2 conditions: Fe^{2+}/H_2O_2 = 1:1, H_2O_2 = 30 mM, 20 min; Fe^{2+}/PMS conditions: Fe^{2+}/PMS = 1:1, PMS = 1 mM, 20 min).

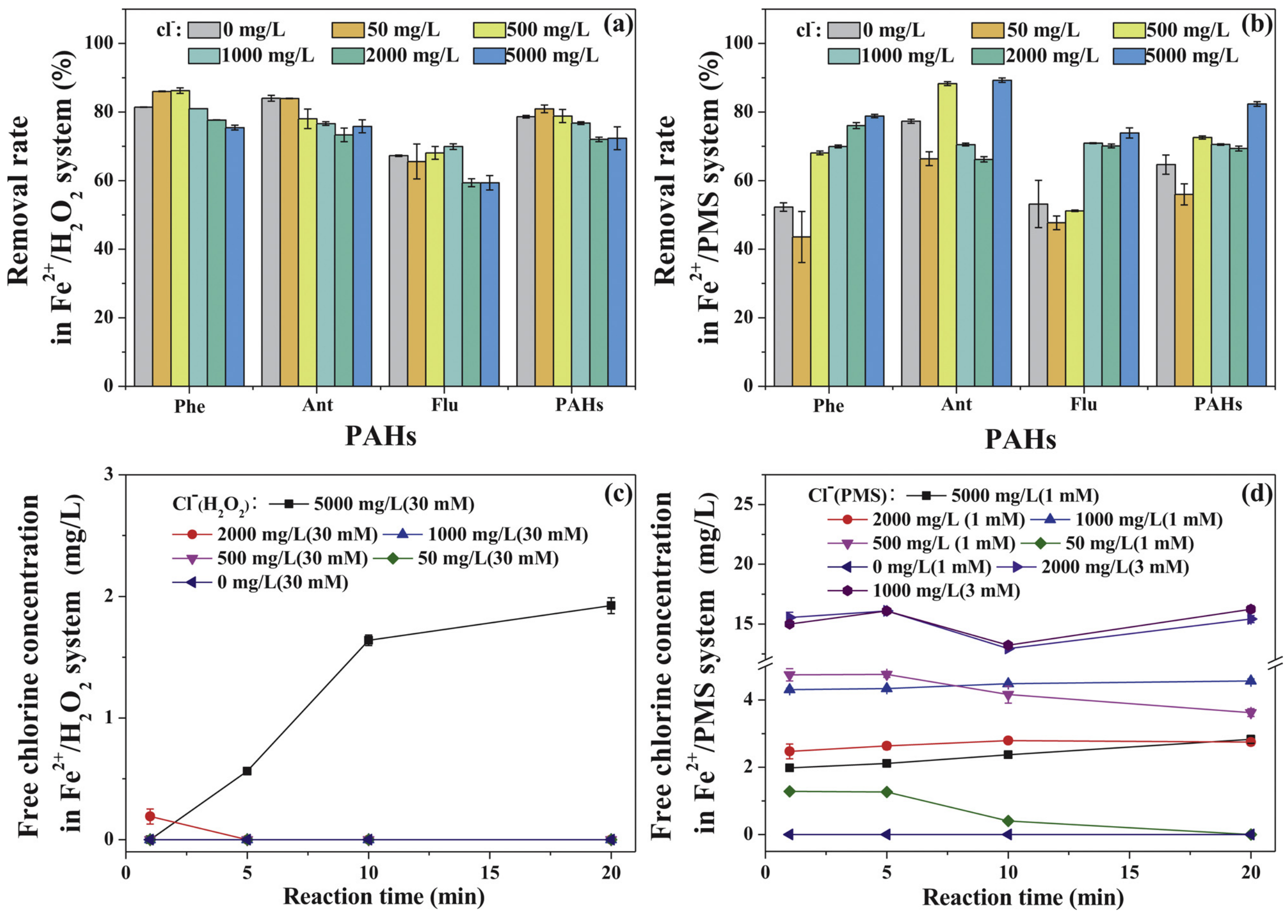

Fig. 5. Effect of the chloride ion concentration on the PAHs removal and free chlorine formation in the Fe^{2+}/H_2O_2 and Fe^{2+}/PMS systems (Fe^{2+}/H_2O_2 conditions: Fe^{2+}/H_2O_2 = 1:1, H_2O_2 = 30 mM, 20 min; Fe^{2+}/PMS conditions: Fe^{2+}/PMS = 1:1, PMS = 1 mM or 3 mM, 20 min).

while the lowest removal rate of the total PAHs (72.01 %–72.37 %) was obtained for the Cl^- concentration of 2000–5000 mg/L. When Cl^- concentration was 5000 mg/L, the removal rates of Phe, Ant, Flu, and total PAHs were 5.96 %, 8.18 %, 7.90 %, and 6.26 % lower than those without Cl^-, respectively. In the Fe^{2+}/PMS system, the removal rates of Phe, Flu, and total PAHs increased with increasing Cl^- concentration—considering the interference of error and Ant removal rate. And when the Cl^- concentration was 5000 mg/L, the removal rates of Phe, Flu, and total PAHs were 78.82 % ± 0.48 %, 73.89 % ± 1.47 %, and 82.35 % ± 0.70 %, respectively. At these conditions, the removal rates of Phe, Flu and total PAHs increased by 10.74 %, 22.69 %, and 9.79 %, respectively, compared to the results obtained without Cl^-. Yang (2015) and Wu et al. (2019) showed that when the Cl^- concentration was from 0 mg/L to 1200 mg/L, the steady-state concentration of $\cdot OH$ in the UV/H_2O_2 system was basically unchanged, while the steady-state concentration of $SO_4^{\cdot -}$ in the UV/persulfacte system decreased by four orders of magnitude. Therefore, Cl^- has a greater influence on $SO_4^{\cdot -}$ and the removal of PAHs by Fe^{2+}/PMS. In this study, for the Cl^- concentration of 2000 mg/L, the removal rates of total PAHs in the Fe^{2+}/H_2O_2 system and the Fe^{2+}/PMS system were 72.01 % ± 0.67 % and 69.37 % ± 0.72 %, respectively. Thus, for the Cl^- concentration of 2000 mg/L, Fe^{2+}/H_2O_2 and Fe^{2+}/PMS showed the same ability to remove PAHs from the simulated sludge. However, the Fe^{2+}/H_2O_2 system was more advantageous for removing the PAHs from the simulated sludge when the sludge contained less than 2000 mg/L Cl^-. In practical applications, chlorine-containing flocculants such as polyaluminum chloride are now increasingly less used due to their poor flocculation efficiency. Therefore, the use of the Fe^{2+}/H_2O_2 system is still a better method for the removal of PAHs from textile dyeing sludge. In addition, according to the analysis of ClO_3^- in the degradation systems, it was found that the $Fe^{2+}/H_2O_2/Cl^-$ and Fe^{2+}/PMS/Cl^- systems will not cause secondary pollution due to ClO_3^- generation in the treatment of textile dyeing sludge (Text S6).

In the $Fe^{2+}/H_2O_2/Cl^-$ system, H_2O_2 reacted with Cl^- to generate free chlorine (Cl_2, HClO, ClO^-) under acidic conditions (Eqs. (1)–(2)), while HSO_5^- in the Fe^{2+}/PMS/Cl^- system reacted with Cl^- to generate free chlorine under neutral conditions (Eqs. (3)–(4)) (Fang et al., 2014; Wu et al., 2019). The obtained results for the concentration of free chlorine in the $Fe^{2+}/H_2O_2/Cl^-$ and Fe^{2+}/PMS/Cl^- systems are shown in Fig. 5(c) and (d). The pH of the liquid phase of the simulated sludge before the reaction was 7.00 ± 0.01, and the pH of the liquid phase of the simulated sludge treated by the $Fe^{2+}/H_2O_2/Cl^-$ (Fe^{2+}/H_2O_2 = 1:1; H_2O_2 = 30 mM; 20 min) and Fe^{2+}/PMS/Cl^- (Fe^{2+}/PMS = 1:1; PMS = 1 mM; 20 min) systems were 2.69 ± 0.26 and 5.19 ± 0.03, respectively. As observed from Fig. 5(c), free chlorine was formed in the $Fe^{2+}/H_2O_2/Cl^-$ system only when the Cl^- concentration was 5000 mg/L. It is also observed that the concentration of free chlorine increased with the increased reaction time. A low concentration of Cl^- could not form free chlorine in the $Fe^{2+}/H_2O_2/Cl^-$ system, possibly due to the strong reduction of H_2O_2 to convert free chlorine into Cl^- (Eq. (5)) (Luo et al., 2019). However, when Cl^- concentration was 5000 mg/L, the free chlorine was not reduced by H_2O_2, possibly due to a large amount of Cl^- consuming a large amount of H_2O_2. As shown in Fig. 5(d), when the Fe^{2+}/PMS system contained Cl^-, free chlorine was generated in the system. This was because HSO_5^- reacted with Cl^- to form free chlorine under a wide pH conditions. The formation of free chlorine in the Fe^{2+}/PMS/Cl^- system was very rapid, and a stable concentration of free chlorine was obtained in a short reaction time. With longer time, the concentration of free chlorine remained essentially unchanged, except for the case of the Cl^- concentration of 50 mg/L. It is highly likely that free chlorine will decompose into chlorine radicals (Eqs. (6)–(7)) (Fang et al., 2014), and therefore, the concentration of free chlorine did not increase with increasing reaction time. Furthermore, for a low Cl^- concentration (50 mg/L), the Cl^- concentration clearly decreased with the increased reaction time, so that the free chloride content decreased with longer reaction time. As the Cl^- concentration increased, the concentration of free chlorine first increased and then decreased. It appears that more Cl^- reacted with $SO_4^{\cdot-}$ to form free radical RCS than free chlorine in the case of high Cl^- concentration. With the increase in the PMS dosage, the concentration of free chlorine increased. When the PMS dosage was increased by a factor of 3 (3 mM), the concentration of free chlorine increased by 2.95–6.29 times. Therefore, the formation of free chlorine in the Fe^{2+}/PMS system was related to the Cl^- concentration and PMS dosage.

$$H_2O_2 + 2HCl \rightarrow Cl_2 + 2H_2O \tag{1}$$

$$H_2O_2 + HCl \rightarrow HClO + H_2O \tag{2}$$

$$HSO_5^- + Cl^- \rightarrow HClO + SO_4^{2-} \tag{3}$$

$$HSO_5^- + 2Cl^- + H^+ \rightarrow Cl_2 + H_2O + SO_4^{2-} \tag{4}$$

$$H_2O_2 + HClO \rightarrow HCl + O_2 + H_2O \tag{5}$$

$$HClO/ClO^- \rightarrow \bullet Cl + \bullet OH/O^{\bullet -} \tag{6}$$

$$Cl_2 \rightarrow \bullet Cl + \bullet Cl \tag{7}$$

Fang et al. (2014) and Wu et al. (2019) showed that Cl^- reacts with $\cdot OH$ and $SO_4^{\cdot-}$ to form free radical RCS ($^{\cdot}Cl$, $Cl_2^{\cdot-}$, $ClO^{\cdot}$). Summarizing the existing reaction equations, the formation and transformation of free radical RCS in $Fe^{2+}/H_2O_2/Cl^-$ and Fe^{2+}/PMS/Cl^- systems are illustrated in Fig. 6. Since it was difficult for the Cl^- at low concentration to form free chlorine in the $Fe^{2+}/H_2O_2/Cl^-$ system, the free radical RCS in $Fe^{2+}/H_2O_2/Cl^-$ system were mainly $\cdot Cl$ and $Cl_2^{\cdot-}$. In the $Fe^{2+}/H_2O_2/Cl^-$ system, the removal of Phe, Flu, and total PAHs first increased and then decreased with the increase in the Cl^- concentration (Fig. 5(a)). It appears that with the increase in the Cl^- concentration, the reaction involving $ClOH^{\cdot-}$ and $\cdot Cl$ to $Cl_2^{\cdot-}$ were accelerated, reducing the $\cdot Cl$ concentration in the degradation system (Fig. 6(a)). Because the free radical RCS is a selective free radical (Hua et al., 2019), the experimental results showed that $\cdot Cl$ had a good selective reaction with Phe and Flu, while $Cl_2^{\cdot-}$ showed the opposite behavior. In the Fe^{2+}/PMS/Cl^- system, the removal rates of Phe, Flu, and total PAHs increased with the increase in the Cl^- concentration (Fig. 5(b)). Gu et al. (2018) showed that the removal of Phe in the aqueous phase by PMS system is improved at higher Cl^- concentration. Thus, both the previous studies and this study proved that free radical RCS has higher reactivity to Phe. In this study, $SO_4^{\cdot-}$ and Cl^- can directly form $^{\cdot}Cl$, while it is difficult for $^{\cdot}OH$ to react with Cl^- to form $ClOH^{\cdot-}$ and then convert into $^{\cdot}Cl$ (Fig. 6), so the $\cdot Cl$ content in the Fe^{2+}/PMS/Cl^- system might be higher than that in the $Fe^{2+}/H_2O_2/Cl^-$ system. Furthermore, the increase in the Cl^- concentration was beneficial not only for the $^{\cdot}Cl$ conversion but also for the $\cdot Cl$ formation and $^{\cdot}OH$ conversion to $\cdot Cl$ (Fig. 6(b)). In the $Fe^{2+}/H_2O_2/Cl^-$ and Fe^{2+}/PMS/Cl^- system, the effect of Cl^- concentration on Ant removal was different from that on Phe and Flu removal. This was probably because the reactivity of free radical RCS with Ant might not be as good as that of $\cdot OH/SO_4^{\cdot-}$ with Ant. But the chlorination of free chlorine removed part of Ant. Thus, the removal rate of Ant varied greatly and irregularly in the Fe^{2+}/PMS/Cl^- system.

3.4. Degradation products of PAHs

3.4.1. Production of total organochlorine

The total organochlorine (TOCl) is an important measure for the determination of chlorinated organics that can quantify the total amount of the chlorinated by-products. Fig. 7 showed the TOCl results obtained in the Fe^{2+}/H_2O_2 and Fe^{2+}/PMS systems under different Cl^- concentrations. The TOCl amounts in the solid phase (simulated sludge) and the liquid phase were almost zero in the $Fe^{2+}/H_2O_2/Cl^-$ system. Only when the Cl^- concentration reached 5000 mg/L, 277.25 ± 7.68 μg/L TOCl was detected in the liquid phase of the $Fe^{2+}/H_2O_2/Cl^-$ system. As reported by Huang et al. (2018), the formation of chlorinated by-products was mainly due to the attack of the chlorine radicals or direct chlorination (electrophilic substitution) by free chlorine on the organic matter itself or its intermediate products. Almost no free chlorine existed in the $Fe^{2+}/H_2O_2/Cl^-$ system, so that PAHs and their intermediate products could not be directly chlorinated by free chlorine to form chlorinated by-products. There were almost no chlorinated by-products in the $Fe^{2+}/H_2O_2/Cl^-$ system, indicating that the effect of $^{\cdot}Cl$ on PAHs and their intermediate products made only a small contribution to the total free radical effect; the steady-state concentration of $^{\cdot}Cl$ in the $Fe^{2+}/H_2O_2/Cl^-$ system might be lower than that in the Fe^{2+}/PMS/Cl^- system. Even if PAHs and their intermediates are chlorinated by $^{\cdot}Cl$ in the $Fe^{2+}/H_2O_2/Cl^-$ system, chlorinated by-products are likely to be degraded by $^{\cdot}OH$.

By contrast, different TOCl concentrations were detected in the Fe^{2+}/PMS system under different Cl^- concentrations (50–5000 mg/L). Moreover, with the increased Cl^- concentration, the TOCl concentration increased significantly in the degradation process of PAHs. This

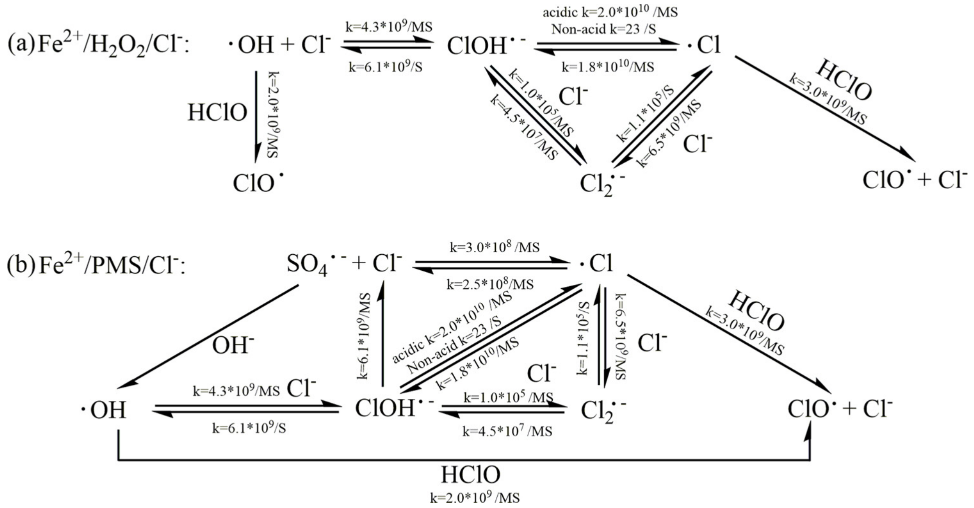

Fig. 6. Generation and conversion of chlorine radical in $Fe^{2+}/H_2O_2/Cl^-$ (a) and Fe^{2+}/PMS/Cl^- (b) systems.

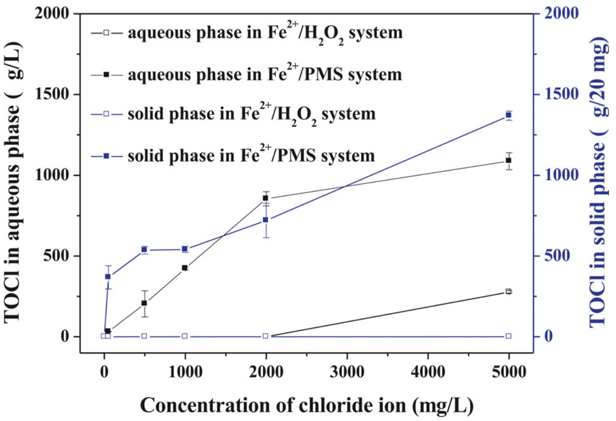

Fig. 7. Effect of chloride ion concentration on the total organic chlorine production in the Fe^{2+}/H_2O_2 and Fe^{2+}/PMS systems (Fe^{2+}/H_2O_2 conditions: $Fe^{2+}/H_2O_2 = 1:1$, $H_2O_2 = 30$ mM, 20 min; Fe^{2+}/PMS conditions: $Fe^{2+}/PMS = 1:1$, PMS = 1 mM, 20 min).

means that with the increase in the Cl^- concentration, the amount of the chlorination by-products increased. As the Cl^- concentration increased from 50 to 5000 mg/L, the TOCl concentration in the liquid phase increased from 32.51 ± 1.10 μg/L to 1087.33 ± 52.92 μg/L, and the TOCl concentration in the solid phase increased from 367.74 ± 71.44 μg/(20 g) to 1367.97 ± 28.23 μg/(20 g). The TOCl concentration in the solid phase was higher than that in the liquid phase, indicating that the chlorinated by-products formed by the degradation of PAHs in the $Fe^{2+}/PMS/Cl^-$ system were mainly hydrophobic organic substances. Since the concentration of free chlorine in the $Fe^{2+}/PMS/Cl^-$ system first increased and then decreased with the increase in the Cl^- concentration, while the TOCl concentration increased monotonically with the increasing Cl^- concentration, the formation of chlorination by-products in the $Fe^{2+}/PMS/Cl^-$ system was not due solely to the chlorination of organic matter and its degradation intermediates by free chlorine. In addition, the correlation between the removal rate of PAHs (Phe, Flu) and TOCl in the $Fe^{2+}/PMS/Cl^-$ system showed that TOCl was significantly correlated with the removal rate of PAHs (the Pearson coefficient for the Phe removal rate and TOCl was 0.834, with p = 0.039, while the Pearson coefficient for the Flu removal rate and TOCl was 0.817, with p = 0.047). Therefore, in the $Fe^{2+}/PMS/Cl^-$ system, the formation mechanism of chlorination by-products was related to the removal mechanism of PAHs. PAHs and their degradation intermediates could also be chlorinated by ·Cl.

3.4.2. Degradation products of Phe, Ant, and Flu

For the simulated sludge containing PAHs (Phe, Ant, Flu) with the concentration similar to that of the actual textile dyeing sludge, the optimal reaction conditions of the Fe^{2+}/H_2O_2 ($Fe^{2+}/H_2O_2 = 1:1$, $H_2O_2 = 30$ mM, 20 min) and Fe^{2+}/PMS ($Fe^{2+}/PMS = 1:1$, PMS = 1 mM, 20 min) systems were determined in this study. The reaction conditions were amplified by a factor of four (the reaction time was unchanged and the Cl^- concentration was 2000 mg/L) to degrade the simulated sludge containing either 1 mg/g Phe or 1 mg/g Ant or 1 mg/g Flu. The degradation products of PAHs (Phe, Ant, Flu) in the $Fe^{2+}/H_2O_2/Cl^-$ or $Fe^{2+}/PMS/Cl^-$ systems were identified by gas chromatography–mass spectrometry (GC–MS) (Fig. 8) and are listed in Table S2. The extracted ion chromatogram of the structures and the corresponding mass spectra of the molecular and fragmented ions are displayed in Figs. S2–S8. The chemical structures of the oxidation products detected by GC–MS were proposed based on the molecular mass, product ion spectra, relative chromatographic retention time, and previously reported information on product formation (Pinto et al., 2014; Xu et al., 2018).

In the $Fe^{2+}/H_2O_2/Cl^-$ system, the removal rates of Phe, Ant, and Flu with high concentration were 39.08 %, 63.46 %, and 49.79 %, respectively, whereas in the $Fe^{2+}/PMS/Cl^-$ system, the removal rates of Phe, Ant, and Flu with high concentration were 66.56 %, 97.19 %, and 86.77 %, respectively. Although the $Fe^{2+}/H_2O_2/Cl^-$ system was not as effective as the $Fe^{2+}/PMS/Cl^-$ system for the removal of high concentration of PAHs, small amounts of oxidation products (1-(4-[2-(4-Methoxymethylphenyl)vinyl]phenyl)ethanone, 4-Hydroxy-3-penten-2-one, 910-Anthracenedione, 3-hydroxyl-fluoranthene) were found in the $Fe^{2+}/H_2O_2/Cl^-$ system. Thus, it was concluded that the $Fe^{2+}/H_2O_2/Cl^-$ system can degrade PAHs more thoroughly than the $Fe^{2+}/PMS/Cl^-$ system.

In the $Fe^{2+}/PMS/Cl^-$ system, 6 types of chlorination by-products were found, and Phe, Ant, and Flu were degraded to form two identical chlorination by-products (trans-1,2-Dichlorocyclopentane, 2-Chlorocyclopentanol). In addition, Phe, Ant, and Flu were chlorinated into the corresponding Cl-PAHs (9-Cl-Phe, 2-Cl-Ant, 9,10-Cl_2-Ant, 3-Cl-Flu). The electron-rich C9 and C10 atoms at the center ring of Phe and Ant were attacked by RCS (free chlorine and free radical RCS) and became 9-Cl-Phe and 9,10-Cl_2-Ant. Moreover, 2-Cl-Ant was also a common Cl-Ant (Johnsen and Gribbestad, 1988; Sankoda et al., 2012), and some studies have shown that Flu can be chlorinated by RCS to form 3-Cl-Flu (Pinto et al., 2014). The $Fe^{2+}/PMS/Cl^-$ system showed a higher PAHs removal ability than the $Fe^{2+}/H_2O_2/Cl^-$ system (Fig. 5(a), (b)), possibly due to the formation of a large number of Cl-PAHs. With the increase in the Cl^- concentration, the removal rate of the PAHs in the Fe^{2+}/PMS system increased due to the chlorination of RCS and oxidation of ·Cl.

In conclusion, in the $Fe^{2+}/H_2O_2/Cl^-$ system, PAHs were oxidized by ·Cl and ·OH, followed by the PAHs ring-opening, and finally became CO_2 and water. However, in the $Fe^{2+}/PMS/Cl^-$ system, there were two pathways for the removal of PAHs: in the first, the PAHs were chlorinated by RCS (˙Cl, Cl_2) to form Cl-PAHs; in the second, the PAHs were oxidized and degraded by ·Cl, ·OH and $SO_4^{\cdot-}$, and some intermediates were chlorinated by RCS (·Cl, Cl_2). The chlorination by-products in the solid phase (simulated sludge) were mainly Cl-PAHs, while the chlorination by-products in the liquid phase were mainly small molecular chlorinated organics. Since after advanced oxidation treatment, the textile dyeing sludge is subjected to the dehydration treatment and then incinerated, the liquid phase will once again enter the wastewater treatment system. Therefore, the chlorination by-products of the solid phase (dehydrated textile dyeing sludge) will enhance the secondary pollution caused by incineration, and the harm caused by the chlorination by-products of the solid phase (dehydrated textile dyeing sludge) was greater than that of the liquid phase. Generally, considering the degradation degree of PAHs, the treatment cost, the formation of chlorination by-products and the whole process, it was concluded that the Fe^{2+}/H_2O_2 system is more advantageous for the treatment of textile dyeing sludge.

4. Conclusion

Advanced oxidation technology based on $SO_4^{\cdot-}$ has been a research hotspot in recent years, and the Fe^{2+}/PMS system may show superior performance to the Fe^{2+}/H_2O_2 system for the removal of PAHs from textile dyeing sludge. The possible replacement of the Fe^{2+}/H_2O_2 system by the Fe^{2+}/PMS system in the textile dyeing sludge treatment was evaluated by analyzing the reagent dosage, PAHs removal, element migration, and chlorination by-product generation. Based on the removal rate of PAHs, the optimal conditions for Fe^{2+}/H_2O_2 or Fe^{2+}/PMS to treat PAHs in the simulated sludge were obtained. The change in the elemental content in the simulated sludge may be related to the attraction and repulsion of ions, the pH of the system, the extent of advanced oxidation, and the amount of the generated iron flocs. Cl^- was not beneficial for the PAHs removal in the Fe^{2+}/H_2O_2 system, because of the low reactivity of $Cl_2^{\cdot-}$ with PAHs, while the opposite was found for the Fe^{2+}/PMS system. In the $Fe^{2+}/PMS/Cl^-$ system, PAHs were

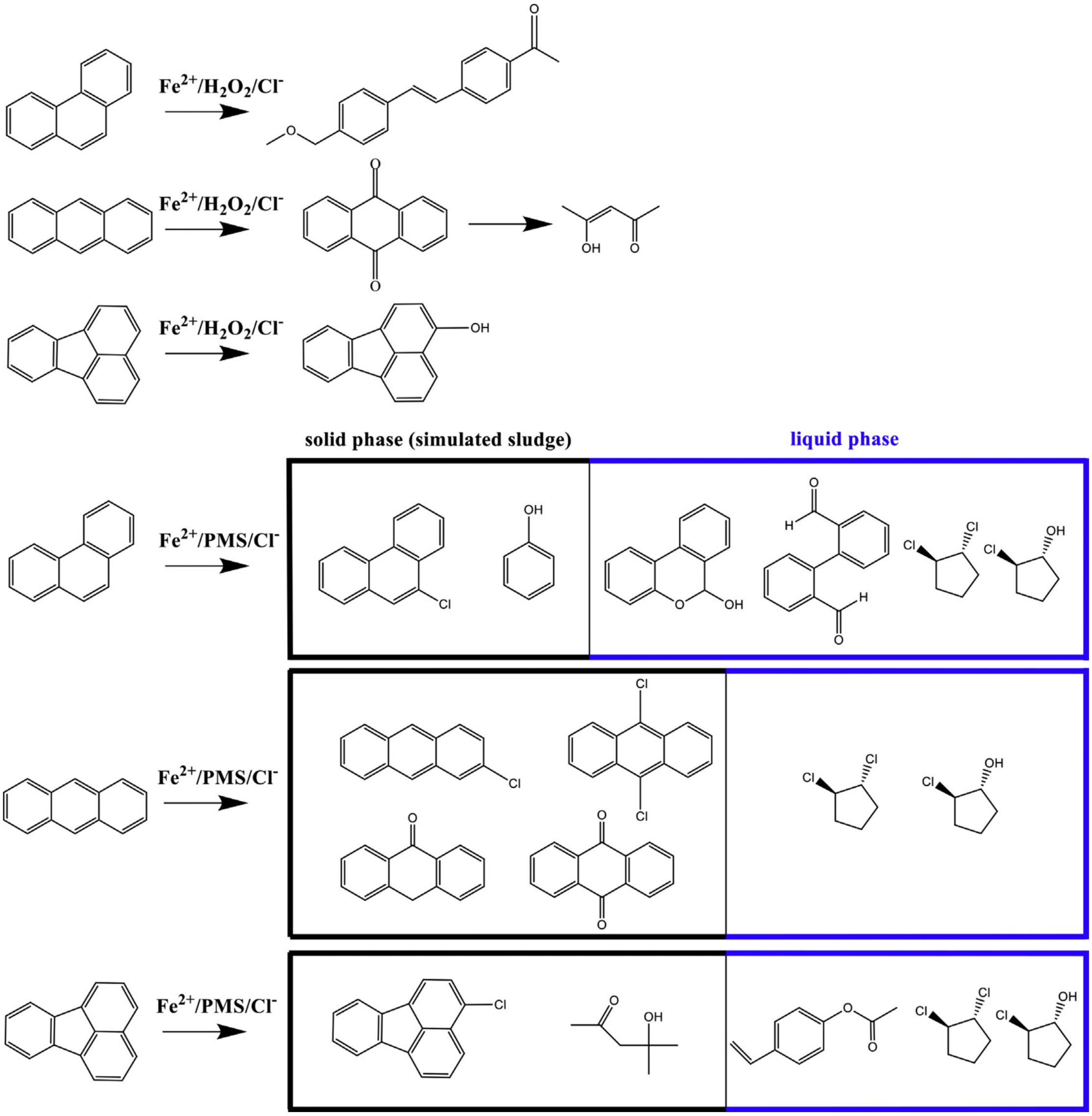

Fig. 8. Degradation products of PAHs (Phe, Ant, Flu) after the $Fe^{2+}/H_2O_2/Cl^-$ or $Fe^{2+}/PMS/Cl^-$ treatment ($Fe^{2+}/H_2O_2/Cl^-$ conditions: Fe^{2+}/H_2O_2 = 1:1; H_2O_2 = 120 mM; reaction time = 20 min; 2000 mg/L Cl^-. $Fe^{2+}/PMS/Cl^-$ conditions: Fe^{2+}/PMS = 1:1; PMS = 4 mM; reaction time = 20 min; 2000 mg/L Cl^-).

degraded into oxidation products by ˙Cl, ·OH and $SO_4^{\cdot-}$, and then PAHs and their oxidation products were chlorinated by ˙Cl and free chlorine, generating a large number of chlorination by-products (e.g. Cl-PAHs). The use of an advanced oxidation method to treat PAHs in textile dyeing sludge and prevention of the formation of toxic and harmful by-products in the degradation process is vital in the treatment of textile dyeing sludge. Therefore, it was concluded that the Fe^{2+}/H_2O_2 system is more suitable for the treatment of textile dyeing sludge. However, considering the whole process of sludge treatment and disposal, the treatment of textile dyeing sludge with the Fe^{2+}/H_2O_2 system poses a risk of enhancing the air pollution in the subsequent sludge incineration. This study provides a basis for obtaining a further understanding of the degradation of PAHs in textile dyeing sludge by the Fe^{2+}/H_2O_2 and Fe^{2+}/PMS systems.

CRediT authorship contribution statement

Xiaojun Lai: Conceptualization, Data curation, Formal analysis, Investigation, Methodology, Software, Writing - original draft. **Xun-an Ning:** Funding acquisition, Project administration, Supervision, Writing - review & editing. **Jiayi Chen:** Investigation. **Yang Li:** Writing - review & editing. **Yaping Zhang:** Writing - review & editing. **Yiqian Yuan:** Investigation, Methodology.

Declaration of Competing Interest

The authors declare that they have no known competing financial interests or personal relationships that could have appeared to influence the work reported in this paper.

Acknowledgments

This work was supported by the Local Innovative and Research Teams Project of Guangdong Pearl River Talents Program [No. 2017BT01Z032], Natural Science Foundation of China [Grant No. 21577027], the 2017 Central Special Fund for Soil, Preliminary Study on Harmless Treatment and Comprehensive Utilization of Tailings in Dabao Mountain [18HK0108].

Appendix A. Supplementary data

Supplementary material related to this article can be found, in the online version, at doi:https://doi.org/10.1016/j.jhazmat.2020.122826.

References

Amand, L.E., Kassman, H., 2013. Decreased PCDD/F formation when co-firing a waste fuel and biomass in a CFB boiler by addition of sulphates or municipal sewage sludge. Waste Manage 33, 1729–1739.

Balcioglu, I.A., Oncu, N.B., Mercan, N., 2017. Beneficial effects of treating waste secondary sludge with thermally activated persulfate. J. Chem. Technol. Biotechnol. 92, 1192–1202.

Beitz, T., Bechmann, W., Mitzner, R., 1998. Investigations of reactions of selected azaarenes with radicals in water. 2. Chlorine and bromine radicals. J. Phys. Chem. A 102, 6766–6771.

Bendouz, M., Tran, L.H., Coudert, L., Mercier, G., Blais, J.F., 2017. Degradation of polycyclic aromatic hydrocarbons in different synthetic solutions by Fenton's oxidation. Environ. Technol. 38, 116–127.

Bissey, L.L., Smith, J.L., Watts, R.J., 2006. Soil organic matter-hydrogen peroxide dynamics in the treatment of contaminated soils and groundwater using catalyzed H_2O_2 propagations (modified Fenton's reagent). Water Res. 40, 2477–2484.

Bolobajev, J., Trapido, M., Goi, A., 2016. Interaction of tannic acid with ferric iron to assist 2,4,6-trichlorophenol catalytic decomposition and reuse of ferric sludge as a source of iron catalyst in Fenton-based treatment. Appl. Catal. B-Environ. 187, 75–82.

Cai, C., Zhang, H., Zhong, X., Hou, L.W., 2014. Electrochemical enhanced heterogeneous activation of peroxydisulfate by Fe-Co/SBA-15 catalyst for the degradation of Orange II in water. Water Res. 66, 473–485.

Cao, B.C., Gao, B.Y., Xu, C.H., Fu, Y., Liu, X., 2010. Effects of pH on coagulation behavior and floc properties in yellow river water treatment using ferric based coagulants. Sci. Bull. 55 (14), 1382–1387.

Fang, J.Y., Fu, Y., Shang, C., 2014. The roles of reactive species in micropollutant degradation in the UV/free chlorine system. Environ. Sci. Technol. 48, 1859–1868.

Forsey, S.P., Thomson, N.R., Barker, J.F., 2010. Oxidation kinetics of polycyclic aromatic hydrocarbons by permanganate. Chemosphere 79, 628–636.

Gang, X., Wang, Q., Qian, Y.J., Gao, P., Su, Y.M., Liu, Z.H., Chen, H., Li, X., Chen, J.B., 2019. Simultaneous removal of aniline, antimony and chromium by ZVI coupled with H2O2: implication for textile wastewater treatment. J. Hazard. Mater. 368, 840–848.

Georgi, A., Reichl, A., Trommler, U., Kopinke, F.D., 2007. Influence of sorption to dissolved humic substances on transformation reactions of hydrophobic organic compounds in water. I. Chlorination of PAHs. Environ. Sci. Technol. 41, 7003–7009.

Gu, M.B., Sui, Q., Farooq, U., Zhang, X., Qiu, Z.F., Lyu, S.G., 2018. Degradation of phenanthrene in sulfate radical based oxidative environment by nZVI-PDA functionalized rGO catalyst. Chem. Eng. J. 354, 541–552.

Guo, K.H., Wu, Z.H., Shang, C., Yao, B., Hou, S.D., Yang, X., Song, W.H., Fang, J.Y., 2017. Radical chemistry and structural relationships of PPCP degradation by UV/chlorine treatment in simulated drinking water. Environ. Sci. Technol. 51, 10431–10439.

Hou, S.D., Ling, L., Dionysiou, D.D., Wan, Y.R., Huang, J.J., Guo, K.H., Li, X.C., Fang, J.Y., 2018. Chlorate formation mechanism in the presence of sulfate radical, chloride, bromide and natural organic matter. Environ. Sci. Technol. 52, 6317–6325.

Hua, Z.C., Guo, K.H., Kong, X.J., Lin, S.K., Wu, Z.H., Wang, L.P., Huang, H., Fang, J.Y., 2019. PPCP degradation and DBP formation in the solar/free chlorine system: effects of pH and dissolved oxygen. Water Res. 150, 77–85.

Huang, Y., Sheng, B., Wang, Z.H., Liu, Q.Z., Yuan, R.X., Xiao, D.X., Liu, J.S., 2018. Deciphering the degradation/chlorination mechanisms of maleic acid in the Fe(II)/peroxymonosulfate process: an often overlooked effect of chloride. Water Res. 145, 453–463.

Johnsen, S., Gribbestad, I.S., 1988. Influence of humic substances on the formation of chlorinated polycyclic aromatic hydrocarbons during chlorination of polycyclic aromatic hydrocarbon polluted water. Environ. Sci. Technol. 22, 978–981.

Lai, X.J., Ning, X.A., He, Y., Yuan, Y.Q., Sun, J., Ke, Y.W., Man, X.Y., 2019. Treatment of a simulated sludge by ultrasonic zero-valent iron/EDTA/Air process: interferences of inorganic salts in polyaromatic hydrocarbon removal. Waste Manage 85, 548–556.

Liang, X., Ning, X.A., Chen, G.X., Lin, M.Q., Liu, J.Y., Wang, Y.J., 2013. Concentrations and speciation of heavy metals in sludge from nine textile dyeing plants. Ecotoxicol. Environ. Saf. 98, 128–134.

Liang, J.Y., Ning, X.A., Song, J., Lu, X.W., Sun, J., Zhang, Y.P., 2019. Treatment of 3,3' -dimethoxybenzidine in sludge by advance oxidation process: degradation products and toxicity evaluation. J. Environ. Manage. 238, 102–109.

Lin, H., Wu, J., Zhang, H., 2014. Degradation of clofibric acid in aqueous solution by an EC/Fe3+/PMS process. Chem. Eng. J. 244, 514–521.

Lin, M.Q., Ning, X.A., An, T.C., Zhang, J.H., Chen, C.M., Ke, Y.W., Wang, Y.J., Zhang, Y.P., Sun, J., Liu, J.Y., 2016. Degradation of polycyclic aromatic hydrocarbons (PAHs) in textile dyeing sludge with ultrasound and Fenton processes: effect of system parameters and synergistic effect study. J. Hazard. Mater. 307, 7–16.

Liu, C.G., Wu, B., Chen, X., 2018. Sulfate radical-based oxidation for sludge treatment: a review. Chem. Eng. J. 335, 865–875.

Luo, C.W., Gao, J., Wu, D.J., Jiang, J., Liu, Y.Z., Zhou, W.W., Ma, J., 2019. Oxidation of 2,4-bromophenol by UV/PDS and formation of bromate and brominated products: a comparison to UV/H2O2. Chem. Eng. J. 358, 1342–1350.

Nganai, S., Lomnicki, S., Dellinger, B., 2009. Ferric oxide mediated formation of PCDD/Fs from 2-monochlorophenol. Environ. Sci. Technol. 43, 368–373.

Ning, X.A., Lin, M.Q., Shen, L.Z., Zhang, J.H., Wang, J.Y., Wang, Y.J., Yang, Z.Y., Liu, J.Y., 2014. Levels, composition profiles and risk assessment of polycyclic aromatic hydrocarbons (PAHs) in sludge from ten textile dyeing plants. Environ. Res. 132, 112–118.

Oncu, N.B., Mercan, N., Balcioglu, I.A., 2015. The impact of ferrous iron/heat-activated persulfate treatment on waste sewage sludge constituents and sorbed antimicrobial micropollutants. Chem. Eng. J. 259, 972–980.

Peluffo, M., Pardo, F., Santos, A., Romero, A., 2016. Use of different kinds of persulfate activation with iron for the remediation of a PAH-contaminated soil. Sci. Total Environ. 563, 649–656.

Pignatello, J.J., Oliveros, E., MacKay, A., 2006. Advanced oxidation processes for organic contaminant destruction based on the Fenton reaction and related chemistry. Crit. Rev. Environ. Sci. Technol. 36, 1–84.

Pinto, M., Rebola, M., Louro, H., Antunes, A.M.M., Jose, S.S., Rocha, M., Silva, M.J., Cardoso, A.S., 2014. Chlorinated polycyclic aromatic hydrocarbons associated with drinking water disinfection: synthesis, formation under aqueous chlorination conditions and genotoxic effects. Polycycl. Aromat. 34, 356–371.

Qin, L.B., Han, J., Chen, W.S., Wang, G.G., Luo, G.Q., Yao, H., 2017. Simultaneous removal of SO2 and PAHs by adding calcium-based additives during sewage sludge incineration in a fluidized bed incinerator. J. Mater. Cycles Waste 19, 1061–1068.

Sankoda, K., Nomiyama, K., Yonehara, T., Kuribayashi, T., Shinohara, R., 2012. Evidence for in situ production of chlorinated polycyclic aromatic hydrocarbons on tidal flats: environmental monitoring and laboratory scale experiment. Chemosphere 88, 542–547.

Waclawek, S., Grubel, K., Dennis, P., Vinod, V.T.P., Cernik, M., 2016. A novel approach for simultaneous improvement of dewaterability, post-digestion liquor properties and toluene removal from anaerobically digested sludge. Chem. Eng. J. 291, 192–198.

Wang, M.H., Xu, L., 2003. General Chemistry. Higher Education Press, Beijing.

Wang, X.H., Li, J.M., Li, X.F., Du, G.C., 2011. Influence of aeration intensity on the performance of A/O-type sequencing batch MBR system treating azo dye wastewater. Front. Environ. Sci. Eng. China 5, 615–622.

Weng, H.X., Ji, Z.Q., Chu, Y., Cheng, C.Q., Zhang, J.J., 2012. Benzene series in sewage sludge from China and its release characteristics during drying process. Environ. Earth Sci. 65, 561–569.

Wu, Y.X., Yang, Y., Liu, Y.Z., Zhang, L.Q., Feng, L., 2019. Modelling study on the effects of chloride on the degradation of bezafibrate and carbamazepine in sulfate radical-based advanced oxidation processes: conversion of reactive radicals. Chem. Eng. J. 358, 1332–1341.

Xu, X., Xiao, R.Y., Dionysiou, D.D., Spinney, R., Fu, T., Li, Q., Wang, Z.J., Wang, D.H., Wei, Z.S., 2018. Kinetics and mechanisms of the formation of chlorinated and oxygenated polycyclic aromatic hydrocarbons during chlorination. Chem. Eng. J. 351, 248–257.

Yang, Y., 2015. Mechanism of the Impact of Inorganic Anions on Typical Organic Contaminant Degradations by $\cdot$OH and $SO_4^{\cdot -}$. Harbin Institute of Technology, China.

Yuan, R.X., Ramjaun, S.N., Wang, Z.H., Liu, J.S., 2011. Effects of chloride ion on degradation of Acid Orange 7 by sulfate radical-based advanced oxidation process: implications for formation of chlorinated aromatic compounds. J. Hazard. Mater. 196, 173–179.

Zhang, Y.J., Gao, Y.X., Zhang, Y., Min, Y., Wang, D.S., Du, C.F., 2005. Study on the hydrolysis process of Fe(III) in Fenton reaction by laser light scattering technology. Environ. Chem. 24 (4), 60 60.

Zhang, G., Hai, J., Ren, M.Z., Zhang, S.K., Cheng, J., Yang, Z.R., 2013. Emission, mass balance, and distribution characteristics of PCDD/Fs and heavy metals during co-combustion of sewage sludge and coal in power plants. Environ. Sci. Technol. 47, 2123–2130.

Zhang, H.D., Gao, Z.P., Ao, W.Y., Li, J., Liu, G.Q., Fu, J., Ran, C.M., Mao, X., Kang, Q.H., Liu, Y., Dai, J.J., 2017. Microwave pyrolysis of textile dyeing sludge in a continuously operated auger reactor: char characterization and analysis. J. Hazard. Mater. 334, 112–120.

Zhu, B.C., 2011. Chemical Reaction Engineering, 5th edition. Chemical Industry Press, China.